

Submicron Patterning of Polymer Brushes: An Unexpected Discovery from Inkjet Printing of Polyelectrolyte Macroinitiators

Adam V. S. Parry,^{†,⊥} Alexander J. Straub,^{†,§,⊥} Eva M. Villar-Alvarez,^{†,||} Takdanai Phuengphol,[‡] Jonathan E. R. Nicoll,[†] Xavier Lim W. K.,[‡] Lianne M. Jordan,[†] Katie L. Moore,[‡] Pablo Taboada,^{||} Stephen G. Yeates,[†] and Steve Edmondson^{*,‡}

[†]The School of Chemistry and [‡]The School of Materials, The University of Manchester, Oxford Road, Manchester M13 9PL, U.K.

[§]Makromolekulare Chemie, Universität Freiburg, Stefan-Meier-Str. 31, 79104 Freiburg, Germany

^{||}Grupo de Física de Coloides y Polímeros, Departamento de Física de la Materia Condensada, 15782-Santuiago de Compostela, Spain

S Supporting Information

ABSTRACT: Using an electrostatic-based super inkjet printer we report the high-resolution deposition of polyelectrolyte macroinitiators and subsequent polymer brush growth using SI-ARGET-ATRP. We go on to demonstrate for the first time a submicron patterning phenomenon through the addition of either a like charged polyelectrolyte homopolymer or through careful control of ionic strength. As a result patterning of polymer brushes down to ca. 300 nm is reported. We present a possible mechanistic model and consider how this may be applied to other polyelectrolyte-based systems as a general method for submicron patterning.

Thin films formed of polymer chains densely end-grafted to a surface are known as polymer brushes.¹ The vast range of chemistries and interesting fundamental properties of polymer brushes has led to emerging applications in diverse fields such as biomedicine, microelectronics, photovoltaics, and sensing.^{2–8} Patterned polymer brushes are finding application in areas such as directing cell growth,⁶ “gecko-mimetic” switchable adhesion,⁹ etch resists, and photonic-based sensors.^{10,11} However, no universal and accessible technique capable of the rapid iteration of high resolution patterns (below 1 μm) over large areas currently exists.^{2,12}

In this contribution we present the inkjet printing of polyelectrolyte macroinitiators^{13–16} (MI) and subsequent polymerization (grafting-from) as an accessible approach to creating polymer brushes. The use of polyelectrolytes for monolayer surface functionalization has several benefits. Spreading on the surface is negligible for these large polymeric molecules, unlike small-molecule thiols,¹⁷ allowing excellent pattern fidelity. Polyelectrolyte deposition can be generalized to any charged surface, avoiding surface-specific and reactive chemical groups¹⁸ and, unlike silane and thiol self-assembled monolayers, polyelectrolytes can be processed from water. Furthermore, these polymers can be synthesized on a large scale, the grafting density (number of initiator sites per unit area) can be tuned through varying monomer ratios, and further functionality can be introduced through copolymerization.

We believe that the digital, on-the-fly and additive nature of inkjet printing has many advantages over conventional approaches for patterning initiator monolayers, which can be subsequently amplified into topographic patterns by other processes. For example, although the commonly used micro-contact printing allows for rapid and complex brush patterning, the initial stamp fabrication usually requires conventional photolithography with a long turnaround time^{19,20} and the generation of submicron features requires more specialized procedures.^{21,22} Furthermore, direct photolithographic monolayer patterning such as the destruction or activation of preformed monolayers suffer from the same barrier to rapid pattern iteration, with lengthy mask fabrication for each new design.^{23–25} There are techniques available that can generate monolayer patterns on-the-fly such as dip-pen nanolithography and e-beam lithography,^{26,27} which are typically used for the production of extremely high resolution patterns; however, these methods require long processing times and can cover only small areas.

The patterning of initiator monolayers by inkjet is a technological challenge, and as such, there are only a few examples in the literature.^{17,28,29} Furthermore, the only demonstration of submicron printing of polymer brushes was achieved by the direct jetting of reactive end-functional polymers using an electrohydrodynamic printer.²⁹ For such grafting-to strategies (direct attachment of preformed polymers to a surface), it is extremely difficult to access high grafting densities and thick brush layers available with a grafting-from approach. In addition, grafting-from allows for the creation of bespoke functionalized thin films of controlled thickness using the vast array of monomers compatible with living polymerization methods.

Here the use of a high-resolution electrostatic-based super inkjet printer (Super Inkjet SIJ-S050) allows fine line patterning of polyelectrolytes from aqueous solutions. The SIJ technology is capable of feature sizes between 1–10 μm, can print a wide range of liquids, and is compatible with different substrates. Further, this work describes the observation of a submicron electrolyte

Received: March 21, 2016

Published: July 11, 2016

induced patterning phenomenon of the MI, enabling features of less than $0.5\ \mu\text{m}$ to be reproducibly fabricated.

All ink formulations used for patterning in this work are based upon a 1:1 v/v mix of water ($18.2\ \text{M}\Omega\cdot\text{cm}$) and ethylene glycol, optimized for SIJ jetting (Supporting Information, SI). Ethylene glycol was chosen as cosolvent as it is completely miscible with water and allows control over surface tension and viscosity. Further, ethylene glycol is known to enhance inward Marangoni flow in aqueous droplets thanks to its high boiling point and low surface tension and is often used to reduce unwanted coffee-stain effects.^{30,31} Cleaned, polished silicon was used as the substrate affording a smooth, flat surface with a negative charge in aqueous solutions for strong attachment of the cationic MI. After printing, the substrates were washed and sonicated in water in order to remove any ungrafted polyelectrolytes from the surface leaving a single polymer monolayer.

The cationic MI copolymer is synthesized using ATRP (see SI) and contains both positively charged side-chains to enable strong electrostatic attraction to the surface and 2-bromoisobutyryl groups to initiate brush polymerization. The MI patterns are amplified by surface initiated atom transfer radical polymerization with activators regenerated by electron transfer (SI-ARGET-ATRP),³² producing robust surface-grafted topographic polymer patterns. The procedure for the polymerization of 2-hydroxyethyl methacrylate (HEMA) has been adapted from previous work (see SI for experimental details).³³ HEMA was chosen as a well investigated system for brush growth. However, the macroinitiator is applicable for a very wide range of other ATRP-compatible monomers and has been demonstrated for pMMA, pNIPAAm, and block copolymers (SI).

Initially patterns were printed using inks that contained only the MI. By careful control of the concentration, washing and polymerization conditions fine lines of pHEMA could be grown with a line width of less than $7\ \mu\text{m}$ (Figure 1). Typical polymer

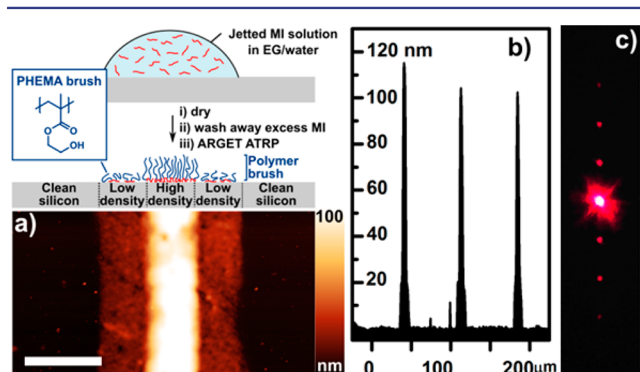


Figure 1. Schematic representation of the deposition of the polyelectrolyte macroinitiator from an aqueous solution and subsequent polymer brush growth. pHEMA was grown on the printed and washed polyelectrolyte macroinitiator monolayers for approximately 2 h followed by characterization with (a) atomic force microscopy (scale bar $5\ \mu\text{m}$) and (b) stylus profilometry (three printed lines). The quality of the printed lines is demonstrated by laser diffraction spots in (c) and further exploited as a basic humidity sensor in the SI.

thickness for 2 h growth time was $100\ \text{nm}$, consistent with dense chain packing in the brush regime and suggesting complete MI coverage of the printed area. The shoulders observed in both the profilometry and the atomic force microscopy images in Figure 1 are a sign of lower grafting density. They are thought to arise from the relatively slow attachment of the MI to the surface compared to the rate of droplet shrinkage during drying. The

success of the MI printing and subsequent polymer brush growth can be seen in a simple diffraction experiment (Figure 1c). The presence of bright diffraction spots around the central reflected one confirms the high quality and repeatability of the patterning. This simple demonstration can be further expanded to create simple humidity sensors thanks to the swelling of pHEMA brushes in the presence of water vapor altering the brightness of the diffracted spots (SI).

The discovery of submicron patterns was a consequence of the addition of a noninitiating homopolymer, poly(2-dimethylamino)ethyl methacrylate methyl chloride quaternary salt (MADQUAT). It is well-known that diluting small molecule initiator monolayers with noninitiating molecules can give reduced and controllable grafting density.³⁴ We have shown that this principle also applied for mixed MI:MADQUAT solutions deposited on surfaces by simple submersion (SI). However, when deposited by inkjet it was found that a preferential deposition of the MI occurred at the contact edge of a printed line, as illustrated in Figure 2. The segregation is

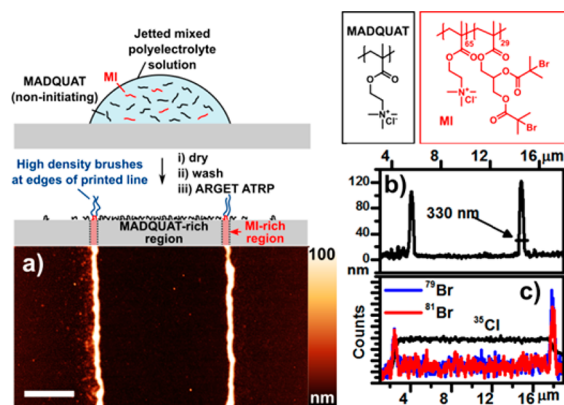


Figure 2. Schematic representation of the deposited and subsequent separation of polyelectrolyte macroinitiator (MI) from the homopolymer MADQUAT leading to the patterning of the grown polymer brushes at the droplet contact edge. pHEMA brushes were grown for approximately 22 h to create lines that were approximately $100\ \text{nm}$ high and less than $500\ \text{nm}$ wide as observed by (a) atomic force microscopy (scale bar $5\ \mu\text{m}$). AFM line profiles of pHEMA brushes (b) reveal the quality of the separation, supported by the NanoSIMS line profile (c), showing the enrichment of Br at the edge of the printed line, the extent of which is shown by the Cl signal arising from both polymers.

easily visualized since pHEMA brush growth by ARGET-ATRP is a selective probe for the presence of initiating 2-bromoisobutyryl groups. Despite the width of the printed line being approximately $8\ \mu\text{m}$, polymer brush lines with submicron widths are produced (Figure 2 and S16).

The MI and the MADQUAT have very similar structures except that the MI contains Br initiating groups on the more hydrophobic comonomer unit. Therefore, bromine signals in NanoSIMS imaging data give further confirmation of the location of the MI monolayer (Figures 2c and S9). Furthermore, the chloride counterion signal can be used to locate both polymers demonstrating the clear separation into a MI-rich region at the edge and a MADQUAT-rich region in the center.

It is tempting to attribute this patterning to a simple example of the well-investigated “coffee-staining” effect, where drying of the drop causes the dissolved material to preferentially deposit at the contact line. However, there are observations that are contrary to this effect, and it is clear that a more subtle mechanism is at work

here. Patterns produced from pure MI inks (Figure 1) show no similar patterning artifacts, suggesting that the solvent system is not responsible for the observed phenomenon. This is further confirmed by profilometry measurements of freshly printed polyelectrolyte film (SI), showing minimal coffee-staining for printed MI:MADQUAT inks before washing. To rule out effects due to the mixed solvent system, inks with pure ethylene glycol and pure water solvents were prepared. The resulting patterns observed after printing and polymerization are very similar to the mixed solvent case (Figures S10 and S17). Patterning is also very similar when using conventional (non-electrostatic) inkjet printing (Figure S17). In addition to simple patterns defined by the edges of printed regions (such as lines and cylinders) more complex patterns such as enclosed boxes are possible due to MI redissolution during multiple prints on one substrate (Figures S18–S21).

The addition of MADQUAT clearly has a significant role to play. By varying the MI:MADQUAT ratio in solution while maintaining overall polymer concentration, we observe a transition to fine, submicron lines as MI:MADQUAT changes from 1:4 to 1:34 w/w% (Figure 3). This suggests that the

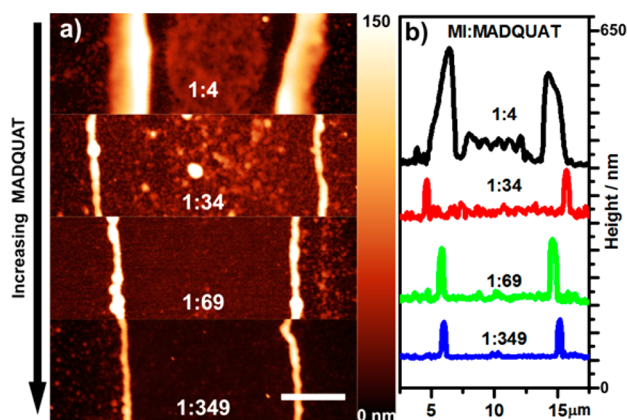


Figure 3. Influence of MI:MADQUAT ratio (w/w%) on the printed polyelectrolyte macroinitiators from (a) atomic force microscopy, scale bar is 3 μm, and (b) line profiles from AFM.

patterning is a consequence of the composition of mixed solutes as opposed to simply a drying drop phenomenon. Furthermore, at very low MI concentrations (1:69 w/w%), almost complete segregation is observed, resulting in the smallest line widths (<500 nm). Moreover, on increasing the amount of MADQUAT further (1:349 w/w%) it is possible to control the grafting density in the MI rich region, as seen by a reduced thickness of pHEMA despite equal polymerization times.

So what is the origin of this segregation? The ink formulation used for printing consists of a mixture of solvents and polyelectrolytes making it an interesting and complex system to analyze. For example, ethylene glycol/water mixtures create internal flows during evaporation due to the differing evaporation rates of the solvents and surface tension gradients. These systems have recently received a great deal of attention due to the observation of droplets of water and food coloring remotely chasing and mixing with one another due to vapor mediated interactions.³⁵ The above observations do, however, suggest a solute-mediated patterning effect.

The complexities of these mixed polyelectrolyte interactions, including with the solvents, between the same polymers and

between different polymers, do present a particular challenge for interpretation.

There are a number of studies of solutions of mixed polyelectrolytes and of polyelectrolytes with added salt, including both practical and theoretical studies.^{36–39} It has been shown that mixed systems that contain polyelectrolytes of similar charge densities generally show good compatibility (miscibility) thanks to dominant long-range electrostatic interactions. However, upon the addition of simple salts (e.g., NaCl),³⁶ the addition of surfactants,³⁹ or when charge densities on the polymers are unequal,³⁸ then the compatibility of the polyelectrolyte mixtures worsen. The equivalence of electrostatic interactions between polymers is broken, either due to screening or inherent charge density difference. Short range interactions (e.g., van der Waals) and the fundamental nature of the polymer backbone then become important and phase separation can occur. Considering the differing Debye screening lengths of the polymers in this study (Table S1), it is clear that polymer electrostatic interactions will not be equivalent, and so, phase separation is likely to be observed. Different charge densities and hydrophobicities of the polyelectrolytes will likely lead to different conformations in solution, further driving separation.

It is hypothesized that as a printed drop, line, or pattern begins to dry, the concentration of the two polyelectrolytes and their associated counterions increases, simultaneously increasing short-range polymer interactions (due to decreased separation between polymers) while decreasing long-range electrostatic interaction due to increasing screening by counterions.³⁷ At a critical concentration the short-range interactions between MI and MADQUAT polymers become dominant, causing them to phase separate (segregate) in solution. This ultimately results in a preferential precipitation of the more hydrophobic polymer, MI, from solution. The precipitation of the MI occurs at the point of maximum evaporation, the contact edge of the droplet. Using solute interactions within a drying drop rather than the solvent mixture to preferentially deposit material to the contact edge presents a fascinating new technique for creating submicron patterns.

To check whether this is a polyelectrolyte effect or simply one of increased ionic strength, solutions containing simple salts such as NaCl and CaCl₂ were investigated. In each case MADQUAT was replaced by simple salts in MI inks. It was observed that a similar segregation could be achieved with the inclusion of these simple salts, consistent with the effect of increasing screening in the mechanism proposed above, and MI precipitation could be enhanced at the contact line (Figures 4, S11, and Figure S12 for NaCl and Figure S13 for CaCl₂). There is significantly greater phase separation of the MI at the contact line with MADQUAT than with simple salts, and a much higher ionic strength is required for a similar observation to be achieved (Figure 4b, ionic strength calculations given in Table S1). Further, similar results are observed when replacing MADQUAT with the polyelectrolyte polydiallyldimethylammonium chloride (pDADMAC) at comparative ionic strengths (Figures 4b and S14). It is concluded that the patterning and precipitation of fine lines at the contact edge is a combination of both ionic repulsion and precipitation with a more subtle polymer intramolecular interaction between the MADQUAT and MI leading to phase separation within the drying drop.

In conclusion, we have presented submicron patterning based on segregative phase separation of polyelectrolytes in a drying drop. Super inkjet (SIJ) technology was used for fine line printing of aqueous polyelectrolyte solutions enabling simple monolayer

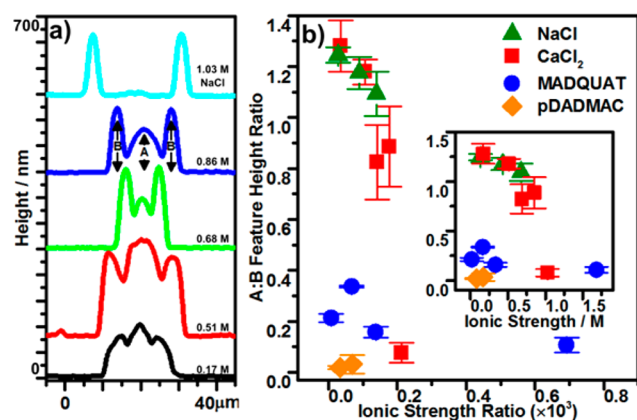


Figure 4. (a) Stylus profilometry of pHEMA brushes from inkjet-printed macroinitiator lines containing $2 \text{ mg}\cdot\text{mL}^{-1}$ of polyelectrolyte macroinitiator and various amounts of NaCl (0.17–1.03 M) from aqueous solutions. (b) Influence of ionic strength on phase separation of MI to the contact edge for NaCl, CaCl_2 , MADQUAT, and pDADMAC, quantified as the ratio of the feature heights A and B against the ratio of ionic strengths of the salt and MI (inset, pure ionic strength of the salt in solution, calculation of ionic strength can be found in Table S1).

patterning onto silicon surfaces. The patterns were amplified by SI-ARGET-ATRP, creating topographic features. This process allows for relatively simple scale up and use with a wide variety of surfaces including polymers and paper. Furthermore, using polyelectrolyte macroinitiators provides a convenient method to visualize the segregation through polymerization. It is likely that this process could be applied to other polyelectrolyte systems, including DNA, RNA, and polysaccharides as a general micropatterning method.

■ ASSOCIATED CONTENT

Supporting Information

The Supporting Information is available free of charge on the ACS Publications website at DOI: 10.1021/jacs.6b02952.

Experimental details and supporting figures (PDF)

■ AUTHOR INFORMATION

Corresponding Author

*stephen.edmondson@manchester.ac.uk

Author Contributions

[†]These authors contributed equally to this work.

Notes

The authors declare no competing financial interest.

■ ACKNOWLEDGMENTS

We thank EPSRC for funding under Strategic Equipment grant EP/L012022/1 and EP/L019728/1 (AVSP). Y. Li and S. P. Armes (Sheffield University, UK) are thanked for the synthesis and donation of the cationic macroinitiator. We would like to thank SIJ Technology and Neil Chilton (Printed Electronics Ltd.) for all their help and support with the SIJ-S050 printer.

■ REFERENCES

- (1) Brittain, W. J.; Minko, S. *J. Polym. Sci., Part A: Polym. Chem.* **2007**, *45*, 3505.
- (2) Barbey, R.; Lavanant, L.; Paripovic, D.; Schüwer, N.; Sugnaux, C.; Tugulu, S.; Klok, H. *Chem. Rev.* **2009**, *109*, 5437.
- (3) Azzaroni, O. *J. Polym. Sci., Part A: Polym. Chem.* **2012**, *50*, 3225.
- (4) Li, B.; Yu, B.; Ye, Q.; Zhou, F. *Acc. Chem. Res.* **2015**, *48*, 229.

- (5) Olivier, A.; Meyer, F.; Raquez, J.-M.; Damman, P.; Dubois, P. *Prog. Polym. Sci.* **2012**, *37*, 157.
- (6) Krishnamoorthy, M.; Hakobyan, S.; Ramstedt, M.; Gautrot, J. E. *Chem. Rev.* **2014**, *114*, 10976.
- (7) Galvin, C. J.; Dimitriou, M. D.; Satija, S. K.; Genzer, J. *J. Am. Chem. Soc.* **2014**, *136*, 12737.
- (8) Liu, H.; Li, Y.; Sun, K.; Fan, J.; Zhang, P.; Meng, J.; Wang, S.; Jiang, L. *J. Am. Chem. Soc.* **2013**, *135*, 7603.
- (9) Chen, J. K.; Wang, J. H.; Fan, S. K.; Chang, J. Y. *J. Phys. Chem. C* **2012**, *116*, 6980.
- (10) Zhou, F.; Liu, W.; Hao, J.; Xu, T.; Chen, M.; Xue, Q. *Adv. Funct. Mater.* **2003**, *13*, 938.
- (11) Zhou, G.-Y.; Lee, A.-W.; Chang, J.-Y.; Huang, C.-H.; Chen, J.-K. *J. Mater. Chem. C* **2014**, *2*, 8226.
- (12) Chen, T.; Amin, I.; Jordan, R. *Chem. Soc. Rev.* **2012**, *41*, 3280.
- (13) Jain, P.; Dai, J.; Grajales, S.; Saha, S.; Baker, G. L.; Bruening, M. L. *Langmuir* **2007**, *23*, 11360.
- (14) Fulghum, T. M.; Estillore, N. C.; Vo, C. D.; Armes, S. P.; Advincula, R. C. *Macromolecules* **2008**, *41*, 429.
- (15) Cheesman, B. T.; Willott, J. D.; Webber, G. B.; Edmondson, S.; Wanless, E. J. *ACS Macro Lett.* **2012**, *1*, 1161.
- (16) Chen, X. Y.; Armes, S. P.; Greaves, S. J.; Watts, J. F. *Langmuir* **2004**, *20*, 587.
- (17) Sankhe, A. Y.; Booth, B. D.; Wiker, N. J.; Kilbey, S. M. *Langmuir* **2005**, *21*, 5332.
- (18) Edmondson, S.; Armes, S. P. *Polym. Int.* **2009**, *58*, 307.
- (19) Xia, Y.; Whitesides, G. M. *Annu. Rev. Mater. Sci.* **1998**, *28*, 153.
- (20) Zhou, F.; Zheng, Z.; Yu, B.; Liu, W.; Huck, W. T. S. *J. Am. Chem. Soc.* **2006**, *128*, 16253.
- (21) Li, H. W.; Muir, B. V. O.; Fichet, G.; Huck, W. T. S. *Langmuir* **2003**, *19*, 1963.
- (22) Odom, T. W.; Love, J. C.; Wolfe, D. B.; Paul, K. E.; Whitesides, G. M. *Langmuir* **2002**, *18*, 5314.
- (23) Steenackers, M.; Küller, A.; Stoycheva, S.; Grunze, M.; Jordan, R. *Langmuir* **2009**, *25*, 2225.
- (24) Panzarasa, G.; Soliveri, G.; Sparnacci, K.; Ardizzone, S. *Chem. Commun.* **2015**, *51*, 7313.
- (25) Fan, X.; Lin, L.; Dalsin, J. L.; Messersmith, P. B. *J. Am. Chem. Soc.* **2005**, *127*, 15843.
- (26) Zapotoczny, S.; Benetti, E. M.; Vancso, G. J. *J. Mater. Chem.* **2007**, *17*, 3293.
- (27) Ballav, N.; Schilp, S.; Zharnikov, M. *Angew. Chem., Int. Ed.* **2008**, *47*, 1421.
- (28) Emmerling, S. G. J.; Langer, L. B. N.; Pihan, S. a.; Lellig, P.; Gutmann, J. S. *Macromolecules* **2010**, *43*, 5033.
- (29) Onses, M. S.; Ramírez-Hernández, A.; Hur, S.; Sutanto, E.; Williamson, L.; Alleyne, A. G.; Nealey, P. F.; de Pablo, J. J.; Rogers, J. A. *ACS Nano* **2014**, *8*, 6606.
- (30) Kuang, M.; Wang, L.; Song, Y. *Adv. Mater.* **2014**, *26*, 6950.
- (31) Kim, D.; Jeong, S.; Park, B. K.; Moon, J. *Appl. Phys. Lett.* **2006**, *89*, 264101.
- (32) Matyjaszewski, K.; Hongchen, D.; Jakubowski, W.; Pietrasik, J.; Kusumo, A. *Langmuir* **2007**, *23*, 4528.
- (33) Zhu, B.; Edmondson, S. *Polymer* **2011**, *52*, 2141.
- (34) Wu, T.; Efimenko, K.; Genzer, J. *J. Am. Chem. Soc.* **2002**, *124*, 9394.
- (35) Cira, N. J.; Benusiglio, a.; Prakash, M. *Nature* **2015**, *519*, 446.
- (36) Stevens, M. J.; Plimpton, S. J. *Eur. Phys. J. B* **1998**, *2*, 341.
- (37) Nishida, K.; Shibata, M.; Kanaya, T.; Kaji, K. *Polymer* **2001**, *42*, 1501.
- (38) Tsubouchi, T.; Nishida, K.; Kanaya, T. *Colloids Surf., B* **2007**, *56*, 265.
- (39) Wills, P. W.; Lopez, S. G.; Burr, J.; Taboada, P.; Yeates, S. G. *Langmuir* **2013**, *29*, 4434.